Shift-variant digital holographic microscopy: inaccuracies in quantitative phase imaging

Ana Doblas,[1] Emilio Sánchez-Ortiga,[1] Manuel Martínez-Corral,[1] Genaro Saavedra,[1] Pedro Andrés,[1] and Jorge Garcia-Sucerquia[1,2,*]

[1]*University of Valencia, 3D Imaging and Display Laboratory, Department of Optics, Burjassot E-46100, Spain*

[2]*Universidad Nacional de Colombia Sede Medellin, School of Physics, A.A: 3840, Medellin 050034, Colombia*

**Corresponding author: jigarcia@unal.edu.co*

Received January 10, 2013; revised February 26, 2013; accepted March 20, 2013; posted March 21, 2013 (Doc. ID 183290); published April 12, 2013

Inaccuracies introduced in quantitative phase digital holographic microscopy by the use of nontelecentric imaging systems are analyzed. Computer modeling of the experimental result shows that even negligible errors in the radius and center of curvature of the numerical compensation needed to get rid of the remaining quadratic phase factor introduce errors in the phase measurements; these errors depend on the position of the object in the field-of-view. However, when a telecentric imaging system is utilized for the recording of the holograms, the numerical modeling and experimental results show the shift-invariant behavior of the quantitative-phase digital holographic microscope. © 2013 Optical Society of America

OCIS codes: 090.1995, 090.1000, 110.0180, 220.1000.

Quantitative phase imaging (QPI) is a required tool for diagnosis and measuring in life and material sciences. This need has driven the development of diverse microscopy methodologies to quantify the phase measurements obtained from micrometer-sized specimens. Methods based on the transport equation [1], the Hilbert transform [2], the diffraction of white light [3], and digital holographic microscopy (DHM) [4,5], are counted among the most utilized. The sensitivity on the phase measurement for some of the above methodologies is in the nanometric range, which allows for testing features on the cell membranes, for instance [5,6].

Because QPI can be utilized for diagnostics of diseases and for refining manufacturing processes, its accuracy is with no doubt a factor to be followed closely. In this Letter is presented an analysis of some possible inaccuracies in QPI-DHM introduced by the optical system used for the recording of the hologram. Computer modeling and experimental results are utilized to show that the use of optical systems with remaining quadratic phase terms introduces inaccuracies in QPI-DHM that it is not possible to remove fully with numerical *a posteriori* approaches.

To perform QPI-DHM, a transmission digital holographic microscope has been built. The setup follows an off-axis architecture by splitting the light from an He–Ne laser with wavelength $\lambda = 633$ nm. The holograms are recorded on a CCD camera with 1024×1024 square pixels of 7 μm side. The wavefield scattered by the object is enlarged over the surface of the CCD to interfere with a tilted reference plane wave. To produce such enlargement an adjustable imaging system is utilized. The latter is composed by a microscope objective (MO) $4x/0.25$ NA and a tube lens (TL) with focal distance $f_{\mathrm{TL}} = 200$ mm; the microscope is illustrated in Fig. 1. For this experimental setup the recorded hologram on the CCD plane is given by

$$H(x,y) = |O|^2 + |R|^2 + OR^* + O^*R, \tag{1}$$

with O and R being the object and reference waves, respectively. For conciseness their (x,y) dependences have been dropped; $*$ stands for the complex conjugate. The digital hologram in Eq. (1) is spatial filtered in the Fourier domain [7] to remove the zero-diffraction order and the twin image. This operation allows for separating the O produced by the imaging system and studying its effects on the reconstructed phase image.

The complex wavefield O produced by the imaging system at the CCD plane can be computed by using regular imaging ABCD transformations [8]. Following this procedure, O is given by

$$O(x,y) = \frac{-1}{M}\exp\left[i\frac{2\pi}{\lambda}(f_{\mathrm{TL}} + f_{\mathrm{MO}} + d)\right] \times \exp\left[i\frac{\pi}{\lambda C}(x^2+y^2)\right] \times \left\{O'\left(\frac{x}{M},\frac{y}{M}\right) \otimes_2 \tilde{P}\left(\frac{x}{\lambda f_{\mathrm{TL}}},\frac{y}{\lambda f_{\mathrm{TL}}}\right)\right\}. \tag{2}$$

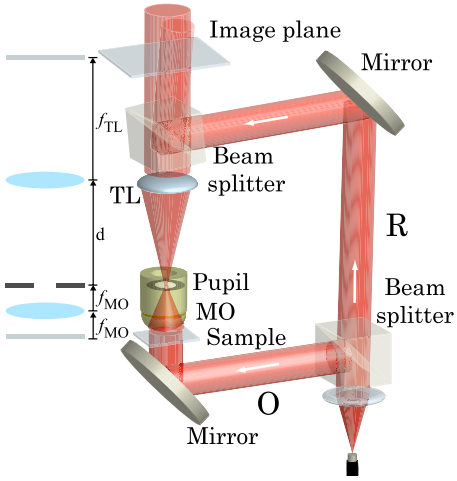

Fig. 1. (Color online) Illustration of the transmission DHM for evaluating the accuracy of the QPI. The MO and TL are utilized for achieving telecentric or nontelecentric operation of the microscope. See text for further details.

$\otimes_2$ represents the two-dimensional convolution between the complex amplitude $O'(\,)$ scattered by the object and the Fourier transform of the aperture function of the imaging system. The magnification of the imaging system $M = -f_{\mathrm{TL}}/f_{\mathrm{MO}}$ is optimized for easing the spatial filtering of the zero-diffraction order and the twin image. Notwithstanding Eq. (2) represents the complex object wavefield imaged in the experimental setup above described, it shows the presence of the quadratic phase factor $\exp[i\pi/\lambda C(x^2 + y^2)]$ that has been recognized in DHM [9,10]; this term is associated with the use of the MO. For our experimental setup the radius of curvature C of this quadratic phase factor is given by

$$C = \frac{f_{\mathrm{TL}}^2}{f_{\mathrm{TL}} - d}, \tag{3}$$

where d is the distance between the MO aperture stop and the TL plane; see Fig. 1. The parameter C can be tuned for resembling the radius of curvature that remains on a typical imaging system built with just the MO. The use of the imaging system presented in this work allows for eliminating fully the additional quadratic phase factor by making $d = f_{\mathrm{TL}}$ [11]; for this configuration the imaging system is telecentric and shift-invariant. For the case $d \neq f_{\mathrm{TL}}$, the presence of the remaining quadratic phase factor turns the DHM into a shift-variant system [12]; hence the accuracy of the QPI-DHM varies according with the specimen position.

Most of the DHM reported in the literature operates in the nontelecentric regimen. In several applications, the remaining quadratic phase factor is eliminated *a posteriori* by means of sometimes intricate numerical approaches [10,13]. Those processes require the accurate computation of the center and radius of curvature of the phase factor to cancel out its effect on the QPI-DHM. However, even a minimal error in these parameters of the quadratic phase factor perturbs the accuracy of the QPI-DHM, as shown below.

Equations (1) and (2) allow for producing a synthetic hologram in which the physical parameters of the setup can be finely controlled. The numerically modeled hologram is then reconstructed following the regular procedure applied to the experimentally recorded measurements. This possibility is utilized to contrast the reconstructed phase images from the experiments with those from the numerically modeled holograms.

A transparent disk with an approximate radius of 690 μm is imaged; the disk has a phase jump of 1.87 rad at a wavelength of 633 nm. To evaluate the performance of the QPI-DHM, the disk is imaged at the very center of the field-of-view (FOV) and at the edge of it. Initially, the system has been set up for operating in nontelecentric mode. This means that there is an offset in the system different from zero; $f_{\mathrm{TL}} - d = 40$ mm offset has been used. The remaining quadratic factor is removed by means of a regular *a posteriori* numerical approach [10,14]. Despite the good qualitative performance of the method, a profile along the center of the disk as it is located at different places on the FOV reveals the remaining shift-variant operation of the DHM. The expected even 1.87 rad phase measurement is slightly distorted at the center and at the edge of the FOV. For both places, there is an upward behavior of the phase measurement. The slope of the phase measurement is higher at the edge than at the center of the FOV; both experimental and numerical modeling results are shown in Fig. 2. The position of the disk at the FOV can be read from the x axis of the plot. The numerical modeling allows for computing approximately the residual error on the *a posteriori* compensation of the quadratic phase factor. The dotted plot is obtained by considering that the correction phase factor is 1 pixel out of center and has an error of 2% on the radius of curvature. These figures are the typical errors that are present in the numerical correction methods.

The inaccuracies described above can be circumvented with the use of telecentric DHM. To demonstrate this, the same experiment was performed but with the DHM operating at null offset. Both the experimental and numerically modeled results are shown in Fig. 3. The solid red (experiment) and dotted blue (numerical model) curves show that for the telecentric DHM the measured phase does not depend on the position of the phase disk. For both positions we measured an average phase jump of 1.74 ± 0.25 rad. The upward behavior of the measured phase in the nontelecentric DHM is no longer present. In other words, the accuracy of the QPI-DHM is maintained for the whole FOV, showing the shift-invariant behavior of the telecentric DHM. The ripples on the experimental measurements correspond to the residual coherent noise, which can be greatly reduced as in [15]. These results show clearly that the use of telecentric DHM is advantageous because (1) it is a shift-invariant imaging system, (2) it does not require *a posteriori* numerical correction of the measured phase, (3) it is a single-shot imaging approach, and (4) it preserves the accuracy of DHM-QPI over the whole FOV.

The complete shift-invariant property that provides the use of the telecentric imaging system in QPI-DHM can be achieved with other methods: by introducing an identical imaging system on the reference arm [16] or by *a posteriori* point-wise subtraction of the measured phase with no sample placed from the measurement with the sample in place [17]. The former is a single-shot approach that requires the very precise alignment of an identical complete imaging system located on the reference

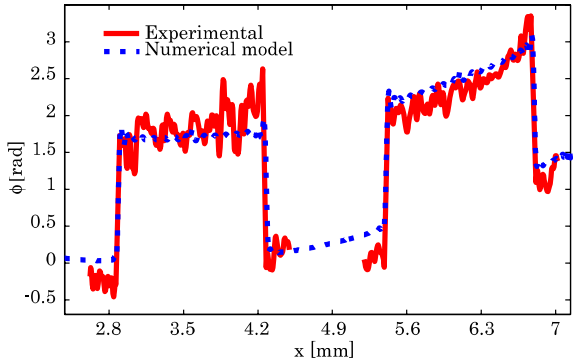

Fig. 2. (Color online) Nontelecentric DHM. Phase profiles along the center of the disk located at different places of the FOV. The solid and dotted curves correspond to experimental and numerical results, respectively.

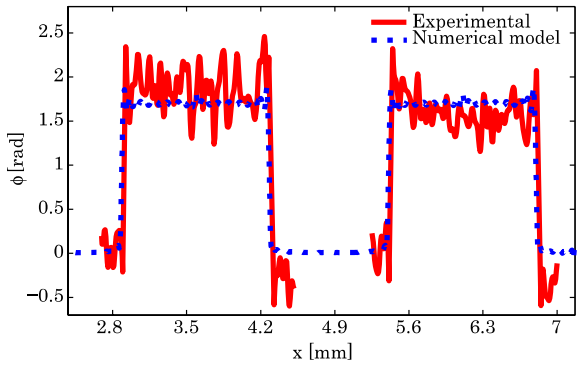

Fig. 3. (Color online) Telecentric DHM. Phase profiles along the center of the disk located at different places of the FOV. The solid and dotted curves correspond to experimental and numerical results, respectively.

arm. The latter needs at least two images to be recorded and processed, which can be complicated for some applications. These reasons support the proposal that telecentric DHM is an ideal approach to have single-shot QPI-DHM.

In summary, in this Letter it has been shown that the accuracy of the QPI measurements performed with DHM can be improved with the use of a telecentric imaging system to record the digital holograms. By means of numerical modeling and experimental results, we show that the shift-variant feature introduced by the nontelecentric imaging system cannot be fully eliminated by the use of numerical *a posteriori* correction approaches. This shift-variant feature perturbs the QPI-DHM measurements of identical objects placed at different positions on the FOV. The numerical modeling of the experimental results shows that even minimal errors in the radius and center of curvature of the numerical compensation of the quadratic phase factor clearly perturb the phase measurements. These results show that the QPI-DHM measurements of an object placed at different positions on the FOV change as their holograms are recorded with a nontelecentric imaging systems. Both numerical modeling and experimental results show that when the holograms are recorded with a telecentric DHM, the lack of presence of the quadratic phase terms allows for performing QPI-DHM measurements with no dependence on the position the specimen of interest within the FOV. This invariance on the QPI-DHM measurement is without any doubt a desired feature for a diagnostic and measuring tool in life and material sciences such as DHM.

This work was supported in part by the Ministerio de Ciencia e Innovación, Spain (Grant DPI2012-32993), and also by Generalitat Valenciana (Grant PROMETEO2009-077). A. Doblas acknowledges a predoctoral fellowship from the University of Valencia. J. Garcia-Sucerquia gratefully acknowledges the Visiting Scholar Fellowship from the Universidad de Valencia, Colciencias grant number 110205024, and UNAL grant numbers 110201003 and 110201004.

References

1. A. Barty, K. A. Nugent, D. Paganin, and A. Roberts, Opt. Lett. **23**, 817 (1998).
2. T. Ikeda, G. Popescu, R. R. Dasari, and M. S. Feld, Opt. Lett. **30**, 1165 (2005).
3. B. Bhaduri, H. Pham, M. Mir, and G. Popescu, Opt. Lett. **37**, 1094 (2012).
4. E. Cuche, F. Bevilacqua, and C. Depeursinge, Opt. Lett. **24**, 291 (1999).
5. P. Marquet, B. Rappaz, P. J. Magistretti, E. Cuche, Y. Emery, T. Colomb, and C. Depeursinge, Opt. Lett. **30**, 468 (2005).
6. G. Popescu, T. Ikeda, K. Goda, C. A. Best-Popescu, M. Laposata, S. Manley, R. R. Dasari, K. Badizadegan, and M. S. Feld, Phys. Rev. Lett. **97**, 218101 (2006).
7. E. Cuche, P. Marquet, and C. Depeursinge, Appl. Opt. **39**, 4070 (2000).
8. D. P. Kelly, J. J. Healy, B. M. Hennelly, and J. T. Sheridan, J. Eur. Opt. Soc. **6**, 11034 (2011).
9. E. Cuche, P. Marquet, and C. Depeursinge, Appl. Opt. **38**, 6994 (1999).
10. T. Colomb, F. Montfort, J. Kühn, N. Aspert, E. Cuche, A. Marian, F. Charrière, S. Bourquin, P. Marquet, and C. Depeursinge, J. Opt. Soc. Am. A **23**, 3177 (2006).
11. E. Sánchez-Ortiga, P. Ferraro, M. Martínez-Corral, G. Saavedra, and A. Doblas, J. Opt. Soc. Am. A **28**, 1410 (2011).
12. D. P. Kelly, B. M. Hennelly, N. Pandey, T. J. Naughton, and W. T. Rhodes, Opt. Eng. **48**, 095801 (2009).
13. K. W. Seo, Y. S. Choi, E. S. Seo, and S. J. Lee, Opt. Lett. **37**, 4976 (2012).
14. T. Colomb, E. Cuche, F. Charrière, J. Kühn, N. Aspert, F. Montfort, P. Marquet, and C. Depeursinge, Appl. Opt. **45**, 851 (2006).
15. J. Kuhn, F. Charriere, T. Colomb, E. Cuche, F. Montfort, Y. Emery, P. Marquet, and C. Depeursinge, Meas. Sci. Technol. **19**, 074007 (2008).
16. C. Mann, L. Yu, C.-M. Lo, and M. Kim, Opt. Express **13**, 8693 (2005).
17. P. Ferraro, S. De Nicola, A. Finizio, G. Coppola, S. Grilli, C. Magro, and G. Pierattini, Appl. Opt. **42**, 1938 (2003).